

Chapter 11

Modeling Absorbers

Here we discuss photoionization modeling and collisional ionization modeling. The collisional ionization part is not yet written.

The goal of modeling the absorbers is to constrain the chemical and ionization conditions of the absorbing gas. From the analysis of the spectral features in the quasars, the absorption line data consist of estimates of the column densities for the ionization stages of several chemical species, $N(x^j)$, where x represents the chemical species and j represents the ionization stage. For example, the MgII $\lambda\lambda 2796, 2803$ doublet provides the column density for the first ionized stage of magnesium, which is written $N(\text{Mg}^{+1})$, and the CIV $\lambda\lambda 1548, 1550$ doublet provides $N(\text{C}^{+3})$, the third ionization stage of carbon.

The ionization fractions, $f(x^j)$, are the ratio of the number density of chemical species x in ionization stage j to the total number density of species x ,

$$f(x^j) = \frac{n(x^j)}{n(x)}, \quad (11.1)$$

where

$$n(x) = \sum_{i=1}^{M_x} n(x^i), \quad (11.2)$$

and where M_x is the number of ionization stages for species x . This quantity is unknown for each species and it can vary with depth in the cloud. Also unknown are the metallicity and abundance pattern of the chemical species. The ionization balance, whether dominated by photoionization or by collisional ionization, also depends most sensitively upon the unknown cloud density and the unknown intensity and shape of the ionizing radiation incident upon the gas cloud.

In practice, the only direct constraints on the model cloud properties are provided by matching the observed column densities, $N(x^j)$, with those obtained by integrating the number densities in the cloud models

$$N_m(x^j) = \int_0^{D_{los}} n(x^j) dl, \quad (11.3)$$

where the integral is over the depth of the model cloud, which is the path length of the line of sight, D_{los} . Often, the coveted column density of neutral hydrogen, N_{HI} , which is especially desirable for constraining metallicity, is not available.

It may seem that attempting to infer these properties from a few measured column densities of a limited number or ionization stages from a handful of chemical species is border-line hubris. However, meaningful constraints often can be placed on the cloud properties, including the cloud sizes and masses.

11.1 Photoionization Modeling

For the assumption of photoionization equilibrium, the industry standard is the code Cloudy, distributed by the Cloudy and Associates group led by Gary Ferland. The code is publicly available at <http://www.nublado.org/>. Here, we outline the general use pattern of Cloudy for quasar absorption line studies.

Standard assumptions are that the model cloud is static (no expansion) with a plane-parallel geometry and unity covering factor. If the hydrogen density, n_{HI} , is assumed to be constant throughout the cloud, then homology relationships can be invoked as a function of several of the other assumed input parameters. This allows flexibility in building model clouds that can then be “scaled” to match observable quantities, such as column densities of various ionization stages of different chemical species.

In Fig. 11.1, a schematic of a Cloudy model is shown. The cloud geometry is assumed to be plane parallel with a constant density n_{HI} and is illuminated on one side (the face) by an ionizing continuum, with spectral energy distribution $J_\nu = J_o f(\nu)$, where J_o is the normalization and $f(\nu)$ represents the continuum shape. The cloud is assumed to have a neutral hydrogen column density N_{HI} , metallicity Z/Z_\odot , and abundance pattern $A(x)$. The parameter U provides the relation between the number density of hydrogen ionizing photons at the cloud face and n_{H} , which is determined by the equilibrium condition of the model.

In the following, we will assume constant density plane parallel “slab” models. The primary model inputs are:

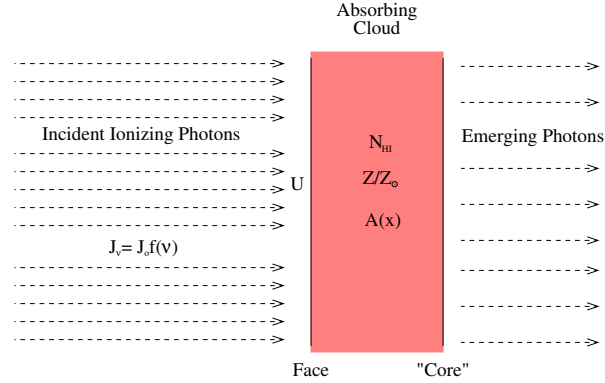


Figure 11.1: — Schematic of a Cloudy model showing the geometric relationship between the cloud face and “core” and the ionizing photon field. The quantities defining the spectral energy distribution of the radiation field, its intensity at the cloud face, and the assumed physical properties of the cloud are explained in the text.

1. The metallicity in solar units, Z/Z_{\odot} , and the abundance pattern, $A(x)$. The abundance pattern can be adjusted to observed astrophysical patterns (options provided by the Cloudy package) or be set arbitrarily. It is common to first assume a solar photospheric abundance pattern and then adjust this accordingly to constraints provided by the data for exploring abundance variations in observed clouds.
2. The spectral energy distribution (SED) of the ionizing photons incident on the cloud face, $f(\nu)$, and the normalization of the SED, J_{ν_0} , at the Lyman edge, $h\nu_0 = 13.6$ eV. For extragalactic absorption systems, it is common to assume the SED expected for the ultraviolet background (UVB). The shape of the SED can significantly alter the ionization balance in the model cloud.
3. The ionization parameter, U , which is the ratio of the number density of hydrogen ionizing photons, n_{γ} , incident on the model cloud face and the hydrogen density, n_{HI} . This parameter is convenient in that it is directly proportional to the SED normalization for a constant density model cloud. U is how the intensity is defined at the face of the model cloud. As U is increased, a given model cloud will be more highly ionized.
4. The neutral hydrogen column density, N_{HI} , of the model cloud. Along with the ionization parameter, U , this is the main input parameter defining the cloud.

For each model cloud, the ionization fractions are determined as a function of depth in the cloud. For optically thin clouds, $\log N_{\text{HI}} \leq 17 \text{ cm}^{-2}$, there is little to no ionization structure. For an optically thick model cloud with a higher N_{HI} , the face of the cloud has higher ionization conditions than the “core”. We write “core” in quotes because the model cloud really has a back side that is not illuminated. The option does exist however, to specify that the ionizing flux is incident on both faces of the model cloud (called “Ly α mode”). Technically, this option simply implements the one-sided model and then, after equilibrium is achieved, reflects the model cloud about the “core”. This results in a doubling of the model’s “observed” column densities.

For quasar absorption line studies, the most applicable output of a Cloudy model is the “observed” column densities of the ionization stage of desired species. These are directly comparable to the actual observed column densities. To expedite the comparison of observed and model column densities, it is common to build a grid of cloud models in both U and N_{HI} for a fixed metallicity and ionizing SED. For example, a grid may consist of 49 cloud models over the range $-4.5 \leq \log U \leq -1.5$ in steps of $\Delta \log U = 0.5$ and $14 \leq \log N_{\text{HI}} \leq 20 \text{ cm}^{-2}$ in steps of $\Delta \log N_{\text{HI}} = 1$.

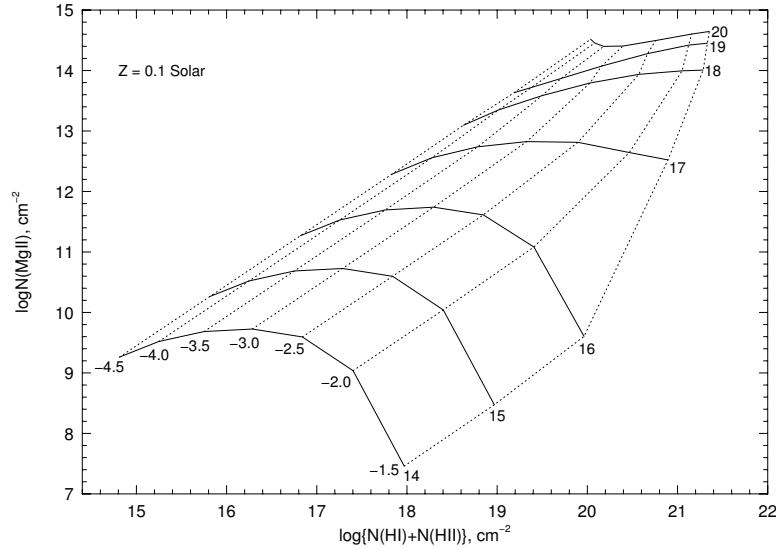


Figure 11.2: — A grid of Cloudy models showing $N(\text{MgII})$ vs. N_{H} for metallicity $Z/Z_{\odot} = 0.1$ and a SED for the UVB at $z = 1$. Solid curves are constant neutral hydrogen column density, N_{HI} , and dotted curves are constant ionization parameter, $\log U$.

In Fig. 11.2, the column density for Mg II is plotted versus the total hydrogen column density, $N_{\text{H I}}$, for a Cloudy photoionization grid. The assumed metallicity is $Z/Z_{\odot} = 0.1$ and the SED is appropriate for a $z = 1$ UVB. Solid curves are constant neutral hydrogen column density, $N_{\text{H I}}$, and dotted curves are constant ionization parameter, $\log U$. The mean ionization fraction of H I for any $(\log U, \log N_{\text{H I}})$ location on the grid can be determined directly from the figure by reading the ratio $N_{\text{H I}}/N_{\text{H}}$.

Because the data are often limited to only one or two ionization states of different chemical species, it can be challenging to constrain both the abundance pattern *and* ionization conditions. Since the ionization balance is sensitive to the SED, there can be a degeneracy between the SED shape and the abundance pattern. If more than one ionization state is observed for a given species, this can help constrain the relationship between the SED and ionization parameter and reduce the degeneracy with abundance pattern. For most quasar absorption line applications, the sensitivity of the SED shape is responsibly explored to help constrain the cloud properties and chemical conditions (abundance pattern) using the the observed data. Thus, a third “dimension” to the grid can be a few to several assumed SEDs.

11.1.1 The Ionization Parameter

The ionization parameter provides the intensity of the ionizing radiation at the face of the model cloud. It is defined as

$$U = \frac{n_{\gamma}}{n_{\text{H}}}, \quad (11.4)$$

where n_{γ} is the number density of hydrogen ionizing photons incident on the face of the cloud, i.e., $h\nu_o \geq 13.6$ eV, and n_{H} is the number density of the total hydrogen (sum of neutral and ionized). In common practice, U is specified as an input to the model and $n_{\text{H I}}$ is obtained from the equilibrium solution. The ionizing photon number density is sensitive to the shape of the spectral energy distribution, J_{ν} , and is given by

$$n_{\gamma} = \int_{\nu_o}^{\infty} \frac{4\pi J_{\nu}}{c} d\nu. \quad (11.5)$$

The term $4\pi J_{\nu}$ is the surface flux of photons [$\text{cm}^{-2} \text{s}^{-1}$] at the cloud face. If the SED has a generalized complex shape, $f(\nu)$, with intensity J_{ν_o} at the Lyman edge of hydrogen,

$$J_{\nu} = J_{\nu_o} f(\nu), \quad (11.6)$$

then the ionizing photon energy can be written

$$n_\gamma = \frac{4\pi}{hc} J_{\nu_o} \int_{\nu_o}^{\infty} \frac{f(\nu)}{\nu} d\nu = \frac{4\pi}{hc} \mathcal{F} J_{\nu_o}, \quad (11.7)$$

where we have defined

$$\mathcal{F} = \int_{\nu_o}^{\infty} \frac{f(\nu)}{\nu} d\nu, \quad (11.8)$$

giving

$$U = \frac{4\pi}{hc} \frac{J_{\nu_o}}{n_{\text{HI}}} \mathcal{F}. \quad (11.9)$$

In the idealized case where the ionizing SED is a power law of the form,

$$J_\nu = J_{\nu_o} \left(\frac{\nu_o}{\nu} \right)^\alpha, \quad (11.10)$$

we have

$$\mathcal{F} = \frac{1}{\alpha}, \quad (11.11)$$

and the ionization parameter can then be expressed,

$$U = \frac{4\pi}{hc} \frac{J_{\nu_o}}{n_{\text{H}} \alpha}, \quad (11.12)$$

where typical values of α are in the range $1 \leq \alpha \leq 2$ for a SED from quasars and AGN.

11.1.2 Model Homology

For the assumed inputs, the model outputs the ionization fractions, $f(x^j)$, of all species as a function of depth in the cloud and the “observed” column densities, $N(x^j)$, integrated through the depth of the cloud for each ionization stage of all species. In optically thin clouds, there is little to no ionization structure with cloud depth. The ionization fractions are constant throughout the cloud.

In optically thick clouds, regions closer to the cloud face will be more highly ionized than those near the cloud “core”. It is important to realize that as the ionizing flux penetrates deeper into the model cloud, the radiation field is hardened (the SED is modified). This follows from the dependence of the photoionization cross section (Eq. 4.12),

$$a_\nu = \sigma_{\nu_o} \left(\frac{\nu_o}{\nu} \right)^3.$$

The highest energy photons have lower probability of participating in an ionization event, and therefore have a longer mean free path through the cloud medium. The result is that species with lower ionization potential have a decreasing probability of being photoionized with increasing depth in the cloud. Thus, there can be significant ionization structure for some species as a function of cloud depth.

11.1.2.1 Metallicity and N_{HI}

For both optically thin and optically thick clouds with a fixed input N_{HI} , U , and SED, the model column density for species x in ionization state j scales linearly with metallicity, following

$$N'(x^j) = N_m(x^j) \left(\frac{Z}{Z_m} \right), \quad (11.13)$$

where $N'(x^j)$ is the “scaled” column density, $N_m(x^j)$ is the model column density, and Z/Z_m is the scaled metallicity with respect to the model metallicity, Z_m . Increasing (lowering) the proportion of a species in every location of the cloud elevates (reduces) the density of all ionization stages of the species.

For optically thin clouds, $\log N_{\text{HI}} < 17 \text{ cm}^{-2}$, there is little to no ionization structure in the model cloud, and the scaling of metallicity is degenerate with a scaling in N_{HI} ,

$$N'(x^j) = N_m(x^j) \left(\frac{N_{\text{HI}}}{N_{\text{HI},m}} \right) \left(\frac{Z}{Z_m} \right), \quad (11.14)$$

where $N_{\text{HI}}/N_{\text{HI},m}$ is the scaled neutral hydrogen column density with respect to the model value, $N_{\text{HI},m}$. In the optically thin regime is especially desirable to have a measure N_{HI} , or an upper limits, perhaps from the lack of a Lyman limit break in the quasar spectrum.

Note that there is no homology relationship for $N'(x^j)$ with $N_{\text{HI}}/N_{\text{HI},m}$ in the regime of optically thick clouds, i.e., $\log N_{\text{HI}} > 17.3 \text{ cm}^{-2}$. In the formalism of Cloudy and the constant density plane-parallel slab model clouds, the addition of N_{HI} to an optically thick cloud is the equivalent of expanding the low ionization “core” of the model cloud, i.e., changing the location of the ionization front. Thus, high ionization stages near the model cloud face will not follow the scaling with $N_{\text{HI}}/N_{\text{HI},m}$.

Depending upon the details of the model cloud, chemical species with very low ionization stages, those with ionization potentials below the Lyman edge, may scale with $N_{\text{HI}}/N_{\text{HI},m}$. For all homology relations, caution is to be exercise in the case of scaling to higher metallicity, especially supersolar levels, because at high metallicity elevated cooling of the electron pool

through recombination to metal species changes the equilibrium temperature and therefore the run of ionization fractions of all species with depth in the cloud. Also, at higher densities, n_{H} , collisional ionization and de-excitation may set in, which also changes the cooling and heating balance (rendering the assumption of equilibrium photoionization invalid).

11.1.2.2 Cloud Densities

Since the normalization of the ionizing SED is not strongly constrained, it is instructive to investigate the dependence of the cloud properties upon J_{ν_o} . Furthermore, since the ionization parameter is often constrained from the data to lie in an “allowed” range, it is also instructive to examine dependence upon U . From Eq. 11.9, we see that the inferred cloud hydrogen number density scales linearly with J_{ν_o} and inversely proportional to U , following

$$n_{\text{H}} = \frac{4\pi}{hc} \frac{J_{\nu_o}}{U} \mathcal{F}. \quad (11.15)$$

Though there is redshift evolution in the value of J_{ν_o} , typical values are roughly on the order of a few to a few tenths in the range $10^{-21} \text{ erg s}^{-1} \text{ cm}^{-2} \text{ Hz}^{-1} \text{ Str}^{-1}$. Typical values of ionization parameters in Lyman limit systems scatter within in an order of magnitude around $U \simeq 10^{-2}$. We have

$$n_{\text{H}} = 6.33 \times 10^{-3} \mathcal{F} \left(\frac{J_{\nu_o}}{10^{-21}} \right) \left(\frac{10^{-2}}{U} \right) \text{ cm}^{-3}, \quad (11.16)$$

where the units of J_{ν_o} are given as above. Since \mathcal{F} is of order unity, we see that typical cloud densities lie in the range $n_{\text{H}} \simeq 0.01 \text{ cm}^{-3}$ and that the density increases (decreases) as the ionization level decreases (increases).

11.1.2.3 Cloud Sizes

The size of the model cloud refers to the linear depth, which observationally corresponds to the length of the line of sight through the cloud, D_{los} . This depth is given by

$$D_{\text{los}} = \frac{N_{\text{H}}}{n_{\text{H}}} = \frac{N_{\text{HI}}}{f_{\text{HI}}} n_{\text{H}}^{-1} \quad (11.17)$$

where N_{H} is the total hydrogen column density,

$$N_{\text{H}} = N_{\text{HI}} + N_{\text{HII}}, \quad (11.18)$$

and where f_{HI} is the ionization fraction of H I,

$$f_{\text{HI}} = \frac{N_{\text{HI}}}{N_{\text{H}}}, \quad (11.19)$$

which can be determined directly from the model. Substituting Eq. 11.15 into D_{los} gives

$$D_{los} = \frac{hc}{4\pi\mathcal{F}} \frac{N_{\text{HI}}}{f_{\text{HI}}} \frac{U}{J_{\nu_o}} \quad (11.20)$$

A typical Lyman limit cloud with unity optical depth has $N_{\text{HI}} = 10^{17.3} \text{ cm}^{-2}$ and an ionization fraction of 1% will have a size of $\simeq 1.5 \text{ kpc}$, and in general

$$D_{los} = \frac{1.6}{\mathcal{F}} \left(\frac{N_{\text{HI}}}{10^{17.3}} \right) \left(\frac{10^{-2}}{f_{\text{HI}}} \right) \left(\frac{U}{10^{-2}} \right) \left(\frac{10^{-21}}{J_{\nu_o}} \right) \text{ kpc}, \quad (11.21)$$

where the units of J_{ν_o} are $\text{erg s}^{-1} \text{ cm}^{-2} \text{ Hz}^{-1} \text{ Str}^{-1}$ and the units of N_{HI} are cm^{-2} .

11.1.2.4 Cloud Masses

To infer the mass of a model cloud, a cloud geometry must be assumed. The model cloud geometry is a plane parallel slab, but to estimate masses, it is common to assume a spherical cloud. Even though this is a grand simplification, it provides a sensible expression for mass estimates. We have

$$M_c = \frac{4\pi}{3} \mu m_{\text{H}} n_{\text{H}} \left(\frac{D_{los}}{2} \right)^3, \quad (11.22)$$

where $\mu = 1.33$ is the mean molecular mass, accounting for the mass fraction of helium, and m_{H} is the mass of hydrogen. Substituting Eqs. 11.15 and 11.20 into M_c gives

$$M_c = \frac{\mu m_{\text{H}} hc}{96\pi\mathcal{F}^2} \left(\frac{N_{\text{HI}}}{f_{\text{HI}}} \right)^3 \left(\frac{U}{J_{\nu_o}} \right)^2. \quad (11.23)$$

For the above assumed fiducial values, the cloud mass is on the order of 10^5 M_{\odot} ,

$$M_c = \frac{1.2 \times 10^5}{\mathcal{F}^2} \left(\frac{N_{\text{HI}}}{10^{17.3}} \right)^3 \left(\frac{10^{-2}}{f_{\text{HI}}} \right)^3 \left(\frac{U}{10^{-2}} \right)^2 \left(\frac{10^{-21}}{J_{\nu_o}} \right)^2 \text{ M}_{\odot}. \quad (11.24)$$

11.2 Collisional Ionization

Not yet written.

References

- Bergeron, J., & Stansínska, G. 1986, “Absorption Line Systems in QSO Spectra: Properties Derived from Observations and from Photoionization Models,” *A&A*, 169, 1
- Churchill, C. W., & Charlton, J. C. 1999, “The Multiple Phases of Interstellar and Halo Gas in a Possible Group of Galaxies at $z \sim 1$,” *AJ*, 118, 59
- Churchill, C. W., Mellon, R. R., Charlton, J. C., & Vogt, S. S. 2003, “The Spatial, Ionization, and Kinematic Conditions of the $z = 1.39$ Damped $\text{Ly}\alpha$ Absorber in Q0957 + 561A,B,” *ApJ*, 593, 203
- Dittman, O. J., & Köppen, J. 1995, “Quasar Absorption Lines: I. The Chemical Composition of the Absorbing Clouds,” *A&A*, 297, 671
- Lauroesch, J. T., Truran, J. W., Welty, D. E., & York, D. G. 1996, “QSO Absorption-Line Systems and EARly Chemical Evolution,” *PASP*, 108, 641
- Steidel, C. C. 1990, “The Properties of Lyman Limit Absorbing Clouds at $z = 3$: Physical Conditions in the Extended Gaseous Halos of High-Redshift Galaxies,” *ApJS*, 74, 37